

Thermodynamics and the Joule-Thomson expansion of dilaton black holes in 2 +1 dimensions

Leonardo Balart¹

*Departamento de Ciencias Físicas,
Facultad de Ingeniería y Ciencias
Universidad de La Frontera, Casilla 54-D
Temuco, Chile.*

Sharmanthie Fernando²

*Department of Physics, Geology & Engineering Technology
Northern Kentucky University
Highland Heights, Kentucky 41099, U.S.A.*

Abstract

In this paper, we study thermodynamics and its applications to the static charged dilaton black hole in 2+1 dimensions. We chose the extended phase space where the pressure $P = -\frac{\Lambda}{8\pi}$. There is a number N for the black hole solutions which leads to a class of black holes where $\frac{2}{3} \leq N < 2$. We noticed that thermodynamic behavior falls into two broad categories: For $\frac{2}{3} \leq N < 1$, the black hole is locally stable for all values of the horizon radius and does not go through phase transitions. For $1 \leq N < 2$, small black holes are locally stable and large black holes are not: there is a first order phase transition between small black holes and the thermal AdS space similar to Hawking-Page phase transition. In order to demonstrate the two broad categories, we have focused on $N = 1$, $\frac{2}{3}$ and $N = \frac{6}{7}$ black holes in detail. We computed the first law and the Smarr relations for the black hole and introduced two new thermodynamical parameters in order to satisfy the first law. We computed specific heat capacities, internal energy and free energy for black holes and studied local and global stability of the black hole. We have also studied the Joule-Thomson expansion for the black hole. It is also noted that unlike the charged BTZ black hole, the charged dilaton black hole does not violate the Reverse Isoperimetric Inequality for certain values of parameters of the theory.

Key words: static, dilaton, black hole, anti-de Sitter space, first law, Smarr relations, Joule-Thomson expansion, Hawking-Page phase transition

1 Introduction

Black hole thermodynamics has been a very active area of research for the past 50 years or so since the seminal work of Bekenstein and Hawking where the relation of entropy to the area at the horizon and temperature at the horizon were discovered [1, 2]. Most interestingly, the work of Hawking and Page on anti-de Sitter black holes, where a first order phase transition between the thermal anti-de Sitter space and the Schwarzschild anti-de Sitter black hole was demonstrated inspired many works on thermodynamics of anti-de Sitter black holes [3]. Another interesting property of anti-de Sitter black

¹leonardo.balart@ufrontera.cl

²fernando@nku.edu

holes is that they have shown to have Van der Waals type phase transitions between small and large black holes. In this case, the cosmological constant is treated as the thermodynamic pressure. Hence the first law of thermodynamics has an extra VdP term and the mass is considered as the enthalpy rather than the internal energy [4, 5]. Many of the AdS black holes has Van der Waals type phase transitions between small and large black holes in this extended phase space. Due to lack of space, we will only mention few examples here: PV criticality of black holes in massive gravity was explored by Fernando in [6]; phase transitions and thermodynamic volume of thermodynamics of rotating black holes and black rings were studies by Altamirano et.al [7]. Exhaustive study of thermodynamics of Born-Infeld black holes were done in [8]. Thermodynamic phase transition of Euler-Heisenberg-AdS black hole on free energy landscape was studied by Dai et.al. in [9]. Few other works along those lines are [10–17]. The reader may read the nice review on thermodynamics of AdS black holes by Kubiznak et.al. [18] to see other examples related to this subject.

Within the framework of the string theory there arises a certain type of scalar field called the dilaton field, which is related to the coupling constant of the string. This field has been coupled with the neutral or electrically (or magnetically) charged BTZ solution [19], which has allowed the construction of various more general solutions [20–30]. Also considering 2+1 dimensional gravity with nonlinear electrodynamics models, Born-Infeld [31], Coulomb-like field [32] and power Maxwell [33], with dilaton fields, new generalizations of the BTZ solution have been obtained in Refs. [34–41], respectively.

The goal of the current paper is to study thermodynamics of charged dilaton black holes in 2+1 dimensions derived by Chan and Mann [20] : here the dilaton field is coupled to the electric field and the cosmological constant via an exponential function. BTZ black hole is one of the solutions of the action considered. Also, for certain parameters of the theory, the corresponding action becomes the low energy string action after a conformal transformation. This family of black hole solutions have very interesting properties and have been studied widely. More details of the properties of this family of solutions will be discussed in the next section.

The paper is organized as follows: in section 2, the charged dilaton black hole in 2+1 dimensions is introduced. Thermodynamics for $\frac{2}{3} < N < 2$ case is presented in section 3. In section 4, thermodynamics for the case $N = \frac{2}{3}$ is presented. Joule Thomson expansion is discussed in section 5. In section 6, Reverse isoperimetric inequality is discussed. Finally the conclusion is given in section 7.

2 Introduction to static charged dilaton black hole in 2+1 dimensions

We consider the Einstein-Maxwell-dilaton action for 2+1-dimensions given by Chan and Mann in Ref. [20]

$$S = \int d^3x \sqrt{-g} \left(R - \frac{B}{2} (\nabla\phi)^2 - e^{-4a\phi} F_{\mu\nu} F^{\mu\nu} - V(\phi) \right), \quad (1)$$

where R is the Ricci scalar, the third term in the parentheses represents the coupling between electrodynamics and the dilaton field ϕ , $F_{\mu\nu}$ is the Maxwell field strength, the dilaton potential is $V(\phi) = 2e^{b\phi}\Lambda$, Λ is the cosmological constant and a , b and B are coupling constant. Here, when $\Lambda < 0$ corresponds to anti-de Sitter space and $\Lambda > 0$ corresponds to the de Sitter space. Notice that in the paper by Chan and Mann [20], $\Lambda > 0$ is treated as the anti-De Sitter case and $\Lambda < 0$ is considered as the de Sitter case. To align our work with most literature on anti-de Sitter black holes, we will consider $\Lambda < 0$. Hence, when Λ appears in our work, it will be a $-\Lambda$ in Chan and Manns work [20].

First, we will present the black hole solutions derived by Chan and Mann in [20]. They considered the following line element,

$$ds^2 = -f(r)dt^2 + f^{-1}(r)dr^2 + r^2 R^2(r)d\theta^2, \quad (2)$$

where

$$R(r) = \gamma r^{\frac{N}{2}-1} \quad (3)$$

and

$$f(r) = -\frac{2mr^{1-\frac{N}{2}}}{N} - \frac{8\Lambda\beta^{2-N}r^N}{(3N-2)N} + \frac{8Q^2}{(2-N)N}. \quad (4)$$

Here γ is a integration constant. Note that the dimensions are: $[r] = L$, $[m] = L^{\frac{N}{2}-1}$, $[\Lambda] = L^{-2}$, $[\beta] = L$, $[Q] = L^0$ and $[\gamma] = L^{1-\frac{N}{2}}$, where L represents units of length. The dilaton field is given by,

$$\phi = k \ln\left(\frac{r}{\beta}\right), \quad (5)$$

where,

$$k = \pm\sqrt{\frac{N(2-N)}{2B}}. \quad (6)$$

The term β represents a constant of integration. Later in the paper β will be presented as a thermodynamic quantity. We will choose $\beta > 0$ since it appears in the $\ln(r/\beta)$ for ϕ in eq.(5).

Notice that N is a dimensionless parameter which leads to a family of black hole solutions. From eq.(6), it is clear that $2 > N > 0$. As discussed in detail by Chan and Mann [20], black hole event horizon exists only for $2 > N > 2/3$ for the metric in eq.(4). For $2/3 > N > 0$ only cosmological horizons exists and will not be discussed in this paper.

If the parameters in the action eq.(1) is chosen to be $b = 4a = 4$ and $B = 8$, the action will be related to string theory by a conformal transformation. It is clear that the above parameters will yield $N = 1$. From $f(r)$ in eq.(4), the black hole gives the metric to the famous MSW charged black hole which is related to string theory [42]. Hence studying thermodynamics of this solution is important

One can observe in eq.(4), there is a singularity at $N = 2/3$ in $f(r)$. This case was not discussed in Chan and Mann's paper. However, Xu [44], derived black hole solutions for $N = \frac{2}{3}$ to be the following metric:

$$f(r) = -\frac{24Mr^{2/3}}{\gamma} - 6\beta^{4/3}\Lambda r^{2/3} \log\left(\frac{r}{\beta}\right) + 9Q^2. \quad (7)$$

Since there are two metric functions depending on the value of N , we will discuss thermodynamics separately for $\frac{2}{3} < N < 2$ and for $N = \frac{2}{3}$ in sections 3 and 4 respectively.

3 Thermodynamics of the black hole for $2/3 < N < 2$

In this paper we are studying thermodynamics in the extended phase space where we consider pressure $P = -\frac{\Lambda}{8\pi}$. In this section we will address thermodynamics of the dilaton black holes for the metric in eq.(2), eq.(3) and eq.(4). First we will replace the mass m with mass M in $f(r)$ with the following relations as given in [45],

$$M = \frac{\gamma m}{8} \quad (8)$$

Then, $f(r)$ is given by,

$$f(r) = -\frac{16Mr^{1-\frac{N}{2}}}{N\gamma} - \frac{8\Lambda\beta^{2-N}r^N}{(3N-2)N} + \frac{8Q^2}{(2-N)N}. \quad (9)$$

We can obtain the entropy using the area law as,

$$S = \frac{2\pi r_+ R(r_+)}{4} = \frac{\pi}{2}\gamma r_+^{N/2}. \quad (10)$$

Considering the fact that $f(r_+) = 0$ we get

$$M = \frac{\gamma}{2}r_+^{\frac{N}{2}-1} \left(-\frac{\Lambda\beta^{2-N}r_+^N}{3N-2} - \frac{Q^2}{N-2} \right). \quad (11)$$

3.1 First law of black hole thermodynamics

It is possible to rewrite the mass M in terms of S, P, Q, β, γ as,

$$M(S, P, Q, \beta, \gamma) = \frac{\pi^{\frac{2}{N}-2}\beta^{-N}S^{-2/N}\gamma^{\frac{2}{N}-2} \left[32\beta^2(N-2)PS^3 - \pi\gamma^2(3N-2)Q^2S\beta^N \right]}{4^{1/N}(N-2)(3N-2)}. \quad (12)$$

We can write the following expression for the first law of thermodynamics as,

$$dM = \left(\frac{\partial M}{\partial S} \right)_{P,Q,\beta,\gamma} dS + \left(\frac{\partial M}{\partial P} \right)_{S,Q,\beta,\gamma} dP + \left(\frac{\partial M}{\partial Q} \right)_{S,P,\beta,\gamma} dQ + \left(\frac{\partial M}{\partial \beta} \right)_{S,P,Q,\gamma} d\beta + \left(\frac{\partial M}{\partial \gamma} \right)_{S,P,Q,\beta} d\gamma, \quad (13)$$

or

$$dM = TdS + VdP + \Phi dQ + \Omega d\beta + \Upsilon d\gamma. \quad (14)$$

Then the temperature can be calculated from the first law of black hole thermodynamics as

$$T = \left(\frac{\partial M}{\partial S} \right)_{P,Q,\beta,\gamma} = \frac{-\Lambda\beta^{2-N}r_+^N - Q^2}{N\pi r_+}. \quad (15)$$

The Hawking temperature obtained using the surface gravity is

$$T_H = \frac{1}{4\pi} \left| \frac{dg_{tt}}{dt} \sqrt{-g^{tt}g^{rr}} \right|_{r_+} = \frac{2M(N-2)r_+^{-N/2}}{\pi N\gamma} - \frac{2\Lambda\beta^{2-N}r_+^{N-1}}{\pi(3N-2)} = \frac{-\Lambda\beta^{2-N}r_+^N - Q^2}{N\pi r_+}, \quad (16)$$

which is equal to T . We also note that the black hole can have degenerate horizons where the temperature is zero; in this case, the degenerate horizon is given by, r_{ex} ,

$$r_{ex}^N = \frac{Q^2}{(-\Lambda\beta^{2-N})} \quad (17)$$

One can obtain the corresponding thermodynamic volume as,

$$V = \left(\frac{\partial M}{\partial P} \right)_{S,Q,\beta,\gamma} = \frac{4\pi\gamma\beta^{2-N}r_+^{\frac{3N}{2}-1}}{3N-2}, \quad (18)$$

which is different from the geometric volume. The electric potential at the horizon is given by

$$\Phi = \left(\frac{\partial M}{\partial Q} \right)_{S,P,\beta,\gamma} = \frac{\gamma Q}{(2-N)r_+^{1-\frac{N}{2}}}. \quad (19)$$

Finally we get the thermodynamic quantity Ω conjugate to the parameter β

$$\Omega = \left(\frac{\partial M}{\partial \beta} \right)_{S,P,Q,\gamma} = \frac{(N-2)\gamma\beta^{1-N}\Lambda r_+^{\frac{3N}{2}-1}}{2(3N-2)}, \quad (20)$$

and the thermodynamic quantity Υ conjugate to the parameter γ

$$\Upsilon = \left(\frac{\partial M}{\partial \gamma} \right)_{S,P,Q,\beta} = \frac{r_+^{\frac{N}{2}-1}}{N} \left(\frac{(N-1)\beta^{2-N}\Lambda r^N}{3N-2} - \frac{Q^2}{N-2} \right). \quad (21)$$

3.2 Smarr formula

Now to obtain the Smarr formula we follow the scaling arguments of Ref. [49]

$$(0)M = (1)\left(\frac{\partial M}{\partial S}\right)S + (-2)\left(\frac{\partial M}{\partial P}\right)P + (0)\left(\frac{\partial M}{\partial Q}\right)Q + (1)\left(\frac{\partial M}{\partial \beta}\right)\beta + \left(1 - \frac{N}{2}\right)\left(\frac{\partial M}{\partial \gamma}\right)\gamma, \quad (22)$$

namely

$$0 = TS - 2VP + \Omega\beta + \left(1 - \frac{N}{2}\right)\Upsilon\gamma. \quad (23)$$

Now, it is necessary to clarify and justify why we consider the terms β and γ as thermodynamic quantities. If we had not done so, then the dimensional analysis of the right side of the Smarr formula will look like $TS - 2VP$ which is not equal to 0. Hence the only way one can develop the first law which is consistent with the Smarr formula is to add the terms $\Omega d\beta$ and $\Upsilon d\gamma$ to the first law of thermodynamics and to include the corresponding terms in the Smarr formula analysis.

3.3 Thermodynamical quantities

We will calculate few more thermodynamical quantities as follows:

$$C_{P,Q} = \frac{N\pi\gamma r_+^{N/2} (\beta^2\Lambda r_+^N + Q^2\beta^N)}{4(N-1)\beta^2\Lambda r_+^N - 4Q^2\beta^N}. \quad (24)$$

Since the enthalpy is given by M , which is equal to $U + PV$, one can compute U as follows:

$$U = M - PV = \frac{\gamma Q^2 r_+^{\frac{N}{2}-1}}{4-2N}. \quad (25)$$

If we write U as a function of temperature T and pressure P , it is,

$$U = -\frac{N\pi\gamma r_+^{\frac{N}{2}} T}{4-2N} + \frac{8\pi\gamma\beta^{2-N} r_+^{\frac{3N}{2}-1} P}{4-2N} \quad (26)$$

Combining eq.(15) and $\Lambda = -8\pi P$, one can obtain the state equation as,

$$P = \frac{NT}{8\beta^{2-N}r_+^{N-1}} + \frac{Q^2}{8\pi r_+^N \beta^{2-N}}. \quad (27)$$

The Gibbs free energy is given by the following expression

$$G = \frac{\gamma r^{\frac{N}{2}-1}}{N} \left(\frac{(N-1)\beta^{2-N}\Lambda r^N}{3N-2} - \frac{Q^2}{N-2} \right). \quad (28)$$

3.4 Maxwell's relations

We can find the Maxwell's relation for thermodynamical quantities from the Helmholtz free energy F . Since $F = U - TS$ and $H = M = U + PV$, one can obtain F as,

$$F = M - PV - TS. \quad (29)$$

Combining dM in eq.(13) with dF from eq.(29), we obtain,

$$dF = -PdV - SdT + \Phi dQ + \Omega d\beta + \Upsilon d\gamma \quad (30)$$

which is equivalent to,

$$dF = \left(\frac{\partial F}{\partial V} \right)_{T,Q,\beta,\gamma} dV + \left(\frac{\partial F}{\partial T} \right)_{V,Q,\beta,\gamma} dT + \left(\frac{\partial F}{\partial Q} \right)_{V,T,\beta,\gamma} dQ + \left(\frac{\partial F}{\partial \beta} \right)_{V,T,Q,\gamma} d\beta + \left(\frac{\partial F}{\partial \gamma} \right)_{V,T,Q,\beta} d\gamma. \quad (31)$$

From the above differential, following relations are obtained:

$$S = - \left(\frac{\partial F}{\partial T} \right)_{Q,\beta,V,\gamma} \quad (32)$$

$$P = - \left(\frac{\partial F}{\partial V} \right)_{T,Q,\beta,\gamma} \quad (33)$$

$$\Phi = \left(\frac{\partial F}{\partial Q} \right)_{T,\beta,V,\gamma} \quad (34)$$

$$\Omega = \left(\frac{\partial F}{\partial \beta} \right)_{T,V,Q,\gamma} \quad (35)$$

$$\Upsilon = \left(\frac{\partial F}{\partial \gamma} \right)_{T,V,Q,\beta} \quad (36)$$

From above four relations, one can differentiate to obtain the following additional 7 relations:

$$- \left(\frac{\partial P}{\partial Q} \right)_{T,\beta,V,\gamma} = \left(\frac{\partial \Phi}{\partial V} \right)_{T,Q,\beta,\gamma} \quad (37)$$

$$- \left(\frac{\partial S}{\partial Q} \right)_{T,\beta,V,\gamma} = \left(\frac{\partial \Phi}{\partial T} \right)_{Q,\beta,V,\gamma} \quad (38)$$

$$\left(\frac{\partial S}{\partial V}\right)_{T,Q,\beta,\gamma} = \left(\frac{\partial P}{\partial T}\right)_{Q,\beta,V,\gamma} \quad (39)$$

$$-\left(\frac{\partial P}{\partial \beta}\right)_{T,Q,V,\gamma} = \left(\frac{\partial \Omega}{\partial V}\right)_{T,Q,\beta,\gamma} \quad (40)$$

$$-\left(\frac{\partial S}{\partial \beta}\right)_{T,Q,V,\gamma} = \left(\frac{\partial \Omega}{\partial T}\right)_{V,Q,\beta,\gamma} \quad (41)$$

$$-\left(\frac{\partial P}{\partial \gamma}\right)_{T,Q,V,\beta} = \left(\frac{\partial \Upsilon}{\partial V}\right)_{T,Q,\beta,\gamma} \quad (42)$$

$$-\left(\frac{\partial S}{\partial \gamma}\right)_{T,Q,V,\beta} = \left(\frac{\partial \Upsilon}{\partial T}\right)_{V,Q,\beta,\gamma} \quad (43)$$

3.5 Comments on the maximum temperature T_{max} and $C_{P,Q}$

Before proceeding to discuss more details on thermodynamics, we would like to make comments on the relation of the temperature and value N as follows: The black hole has a maximum temperature T_{max} at,

$$r_{max}^N = \frac{Q^2}{(N-1)\beta^{2-N}\Lambda} \quad (44)$$

Since $\Lambda < 0$, r_{max} will be real only if $N < 1$. Hence for $2/3 < N < 1$, the maximum temperature is given by,

$$T_{max} = \frac{Q^2}{\pi(1-N)r_+} \quad (45)$$

When $N \geq 1$, the temperature does not have a maximum. In Fig.(1), temperature is plotted for various values of N and one can see that for $N < 1$ there are maximum values of the temperature.

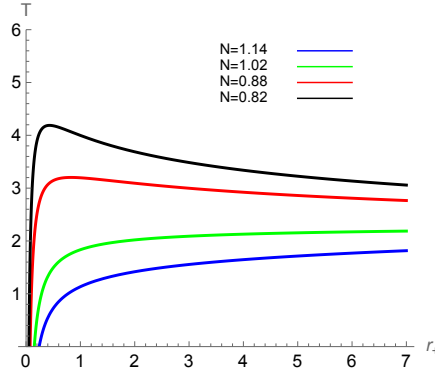


Figure 1: The figure shows the temperature T vs the horizon radius r_+ for varying values of N . Here $Q = 1, \beta = 12.88, -\Lambda = -0.562$.

Existence of a maximum for the temperature does have an effect on the $C_{P,Q}$. Since $C_{P,Q} = T \left(\frac{\partial S}{\partial T}\right)_P$ which is also equal to $T \left(\frac{\partial S}{\partial r_+}\right)_P / \left(\frac{\partial T}{\partial r_+}\right)_P$, existence of the maximum of the temperature does

significantly effects the behavior of $C_{P,Q}$. Since $\left(\frac{\partial T}{\partial r_+}\right) = 0$ at T_{max} , $C_{P,Q} \rightarrow \pm\infty$ at $r = r_{max}$. Hence there would be two branches for $C_{P,Q}$ when T_{max} exists where as there will be only one branch when T_{max} does not exist. This phenomenon is demonstrated in Fig.(2).

We will discuss the details of $C_{P,Q}$ in more depth and detail for the following two examples: we have chosen to describe thermodynamic stability of a black hole with $N = 6/7$ and one with $N = 1$ which represents black holes with a maximum temperature and one without.

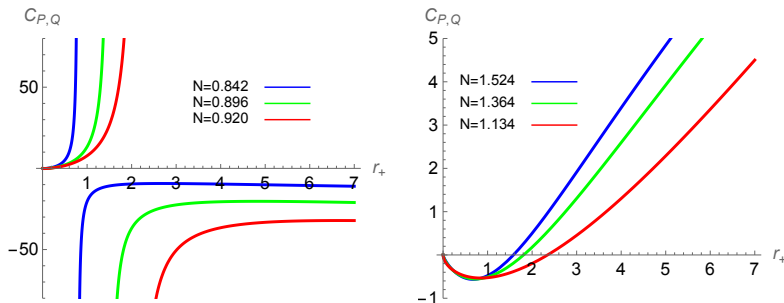


Figure 2: The figure shows the temperature $C_{P,Q}$ vs the horizon radius r_+ for varying values of N . Left graph is for $N < 1$ and the right graph is for $N > 1$. Here $-\Lambda = -0.1, \gamma = 1$ for both graphs. For the left graph, $Q = 0.5, \beta = 17$ and for the right graph $Q = 0.386, \beta = 0.5$

3.6 Thermodynamics for the black hole with $N = \frac{6}{7}$

Here we will analyze details of thermodynamics for the black hole with $N = \frac{6}{7}$. Notice that $\Lambda < 0$ for black hole horizons to exist. As discussed in [20], it is possible to choose M and Q such that there are two horizons, degenerate horizons or none. In the extreme case,

$$Q^2 = \frac{4096}{9261} \left(\frac{M^3}{\beta^{16/7} \gamma^3 \Lambda^2} \right) = aM^3. \quad (46)$$

Here,

$$a = \frac{4096}{9261} \left(\frac{1}{\beta^{16/7} \gamma^3 \Lambda^2} \right). \quad (47)$$

If $Q^2 < aM^3$, one will have a black hole solution and if $Q^2 > aM^3$, then one will have a naked singularity. In Fig.(3) we have plotted $f(r)$ for three values of M for fixed Q . Notice that the relation given for extreme black hole is different from the one given by Chan and Mann [20] since we have redefined mass M in this paper.

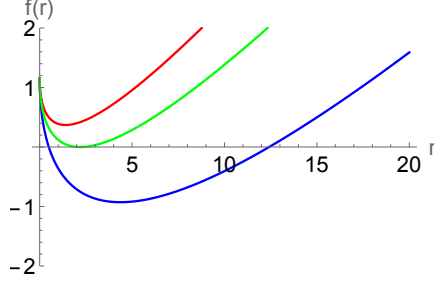


Figure 3: The figure shows $f(r)$ vs r for the dilaton black hole for $N = \frac{6}{7}$. Here $Q = 0.376, \beta = 0.1, \gamma = 1, \Lambda = -1$. The blue curve corresponds to $M = 0.144$ and is a black hole solution with two horizons. The red curve corresponds to $M = 0.104$ and does not have horizons. The green curve corresponds to an extreme black hole with $M = 0.118$.

The pressure P vs r_+ is plotted in Fig.(4). As is clear from the figure, there is a minima for pressure at $r_p = \frac{7Q^2}{\pi T}$. Hence for a given black hole,

$$P > \frac{1}{8\beta^{8/7}} \left(\frac{7}{\pi}\right)^{1/7} \left(\frac{Q^2}{T}\right)^{1/7}. \quad (48)$$

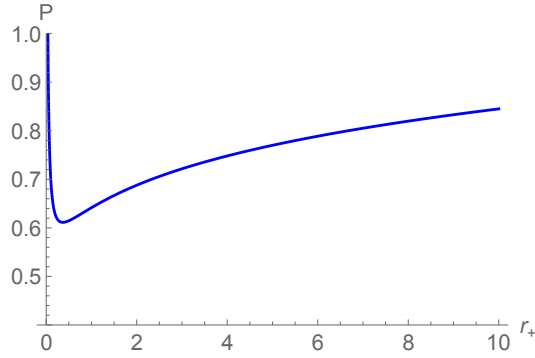


Figure 4: The figure shows the pressure P vs the horizon radius r_+ for fixed charge. Here $N = 6/7, Q = 0.259, T = 0.406$ and $\beta = 0.1$.

3.6.1 Thermodynamic stability

For the black hole to be locally stable, $C_{P,Q} > 0$. We have plotted $C_{P,Q}$ vs r_+ and T vs r_+ in Fig.(5) and Fig.(6). Both T and $C_{P,Q}$ are zero when the black hole is extreme at

$$r_{ex} = \left(\frac{-Q^2}{\beta^{8/7}\Lambda}\right)^{7/6} \quad (49)$$

Temperature T has a local maxima at r_{max} given by,

$$r_{max} = 7^{(7/6)} \left(\frac{-Q^2}{\beta^{8/7}\Lambda} \right)^{7/6} \quad (50)$$

$C_{P,Q} \rightarrow \infty$ when $r = r_{max}$ and beyond that $C_{P,Q} < 0$. Hence, $C_{P,Q} > 0$ between r_{ex} and r_{max} and black holes are locally stable in this region.

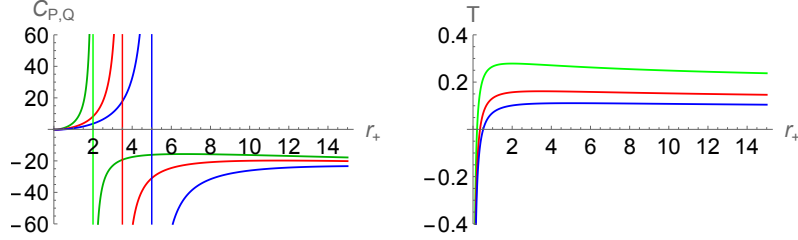


Figure 5: The figure shows the specific heat capacity $C_{P,Q}$ and Hawking temperature T vs the horizon r_+ for fixed charge. Here $N = 6/7$, $Q = 0.5$, $\Lambda = -1$, $\gamma = 1$, and $\beta = 0.97, 0.644, 0.486$ (green, red and blue).

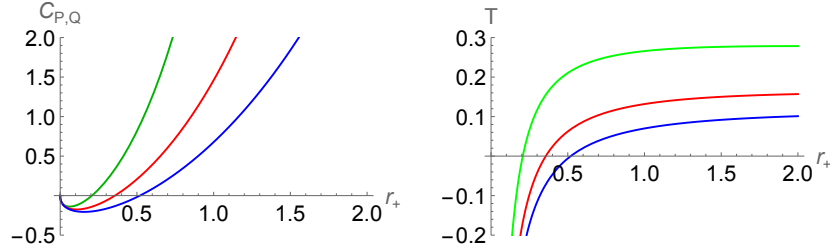


Figure 6: The figure shows the specific heat capacity $C_{P,Q}$ and Hawking temperature T vs the horizon r_+ with amplified scale close to $r_+ = 0$ for the same cases as in Fig.(5).

To understand global stability of a black hole one has to study Gibbs free energy. In the case for $N = \frac{6}{7}$, we have plotted G vs T in Fig.(7). We have plotted G vs r_+ and T vs r_+ in Fig.(8). As demonstrated in Fig.(1) and eq.(50), the temperature T has a maximum, T_{max} . When $T > T_{max}$, no black hole can exist. Hence, for $T > T_{max}$, thermal AdS space is preferred thermodynamically. For $T < T_{max}$ there are two branches of black holes: one corresponds to small black hole with smaller (positive) Gibbs free energy and the other corresponds to large black hole with large still positive free energy. Smaller black holes are locally stable and larger black holes are locally unstable. Given the smaller black hole has lower Gibbs free energy it is the preferred thermodynamical state for $T < T_{max}$. There is a first order phase transition between the AdS space and the smaller black holes at $T = T_{max}$. This is very similar to the Hawking-Page phase transition occurred in the Schwarzschild-AdS black hole [3].

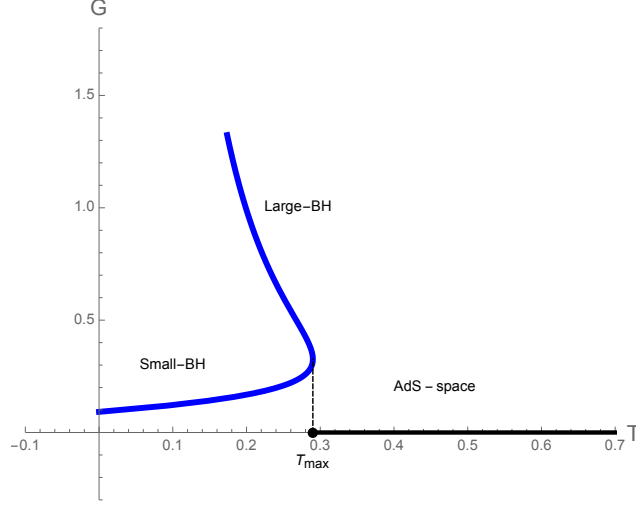


Figure 7: The figure shows the Gibbs free energy G vs the temperature T for fixed charge. Here $N = \frac{6}{7}$, $Q = 0.5$, $\Lambda = -1$, $\gamma = 1$, and $\beta = 1$.

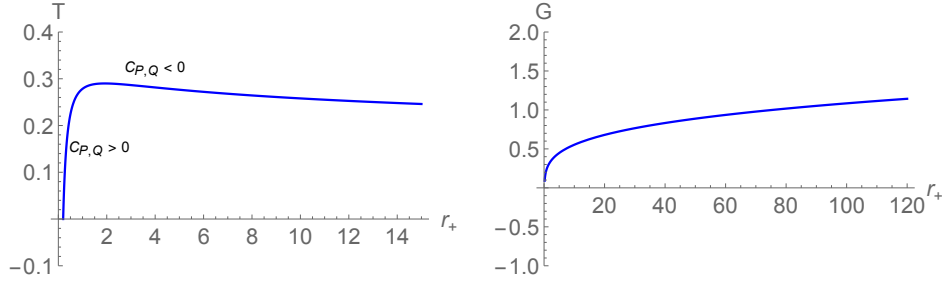


Figure 8: The figure shows the temperature T vs r and Gibbs free energy G vs r for fixed charge. Here $N = \frac{6}{7}$, $Q = 0.5$, $\Lambda = -1$, $\gamma = 1$, and $\beta = 1$.

3.7 Thermodynamics of the black holes for $N = 1$ case

If $N = 1$ in eq.(9), we obtain the black hole solution given by following metric:

$$ds^2 = -f(r)dt^2 + f^{-1}(r)dr^2 + r^2 R^2(r)d\theta^2, \quad (51)$$

where

$$R(r) = \gamma r^{-1/2} \quad (52)$$

and

$$f(r) = \frac{-16M\sqrt{r}}{\gamma} - 8\Lambda\beta r + 8Q^2. \quad (53)$$

The black hole has two horizons given the mass $M > \gamma Q \sqrt{-\beta \Lambda}$. According to eq.(10) in this case, the entropy is given by:

$$S = \frac{2\pi r_+ R(r_+)}{4} = \frac{\pi}{2} \gamma \sqrt{r_+}. \quad (54)$$

3.7.1 First law of black hole thermodynamics and the Smarr formula for $N = 1$

Substituting $N = 1$ into eq.(11) allows us to obtain

$$M(S, P, Q, R) = \frac{\pi \gamma^2 Q^2}{4S} + 8PS\beta. \quad (55)$$

By means of eq.(55) or replacing $N = 1$ in the quantities obtained in subsection 3.1, we derive the following expression for the first law of thermodynamics

$$dM = \left(\frac{\partial M}{\partial S} \right)_{P,Q,\beta} dS + \left(\frac{\partial M}{\partial P} \right)_{S,Q,\beta,\gamma} dP + \left(\frac{\partial M}{\partial q} \right)_{S,P,\beta,\gamma} dQ + \left(\frac{\partial M}{\partial \beta} \right)_{S,P,Q,\gamma} d\beta + \left(\frac{\partial M}{\partial \gamma} \right)_{S,P,Q,\beta} d\gamma, \quad (56)$$

or

$$dM = TdS + VdP + \Phi dQ + \Omega d\beta + \Upsilon d\gamma, \quad (57)$$

where the temperature, volume and electric potential are as follows, respectively

$$T = \left(\frac{\partial M}{\partial S} \right)_{P,Q,\beta,\gamma} = -\frac{Q^2}{\pi r_+} - \frac{\Lambda\beta}{\pi}. \quad (58)$$

$$V = \left(\frac{\partial M}{\partial P} \right)_{S,Q,\beta,\gamma} = 4\pi\beta\gamma\sqrt{r_+}, \quad (59)$$

$$\Phi = \left(\frac{\partial M}{\partial Q} \right)_{S,P,\beta,\gamma} = \frac{\gamma Q}{\sqrt{r_+}}. \quad (60)$$

The thermodynamic quantities Ω and Υ , conjugated to the parameter β and γ respectively, are

$$\Omega = \left(\frac{\partial M}{\partial \beta} \right)_{S,P,Q,\gamma} = -\frac{1}{2}\gamma\Lambda\sqrt{r_+}, \quad (61)$$

and

$$\Upsilon = \left(\frac{\partial M}{\partial \gamma} \right)_{S,P,Q,\beta} = \frac{Q^2}{\sqrt{r_+}}. \quad (62)$$

Notice that when the black hole is extreme, then $T = 0$. Also when $r_+ \rightarrow \infty$, $T \rightarrow -\frac{\Lambda\beta}{\pi}$. There are no local minima or maxima for T . Hence black holes cannot exist for $T < 0$ or $T > -\frac{\Lambda\beta}{\pi}$. Fig.(10) shows the behavior of T vs r_+ for $N = 1$ case.

We also want to note that volume V given by eq.(59) is different from the geometric volume πr_+^2 , and that the charge Q is related to the electric charge Q_{BTZ} of the BTZ black hole [19, 48] as follows from Ref. [45]

$$Q_{BTZ} = \frac{\gamma Q}{2}. \quad (63)$$

The Smarr formula is achieved by either considering $N = 1$ in Eq.(23) or using the results obtained above following the scaling arguments of Ref. [49]. Either way leads us to

$$0 = TS - 2VP + \Omega\beta + \frac{1}{2}\Upsilon\gamma. \quad (64)$$

3.7.2 Other thermodynamical quantities

We will calculate few more thermodynamical quantities, $C_{P,Q}$, $C_{V,Q}$ and internal energy U of the black hole as follows:

$$C_{P,Q} = T \left(\frac{\partial S}{\partial T} \right)_P = \frac{\pi\gamma\sqrt{r_+}(-Q^2 + 8\pi\beta Pr_+)}{4Q^2\beta} \quad (65)$$

the same result is obtained from Eq.(24), and

$$C_{V,Q} = T \left(\frac{\partial S}{\partial T} \right)_V = 0, \quad (66)$$

since when volume is kept constant, i.e. r_+ is kept constant, S does not change. Since the enthalpy is given by M , which is equal to $U + PV$, one can compute U as follows:

$$U = M - PV = \frac{\gamma Q^2}{2\sqrt{r_+}}. \quad (67)$$

If we write U as a function of temperature T , volume V and pressure P , it is,

$$U = -\frac{VT}{8\beta} + PV. \quad (68)$$

If we write U as a function of V, Q, β, γ , then,

$$U = \frac{2\pi\beta\gamma^2 Q^2}{V}. \quad (69)$$

As it can be observed, the internal energy depends on both the temperature and the pressure. In an ideal gas, the internal energy only depends on temperature.

Helmholtz free energy is

$$F = U - TS = \frac{2\pi\beta\gamma^2 Q^2}{V} - \frac{TV}{8\beta}. \quad (70)$$

One can substitute $\Lambda = -8\pi P$ in eq.(58) to obtain the state equation as,

$$P = \frac{T}{8\beta} + \frac{Q^2}{8\pi\beta r_+}. \quad (71)$$

The pressure P is plotted vs r_+ in Fig.(9) below to demonstrate that there are no critical points.

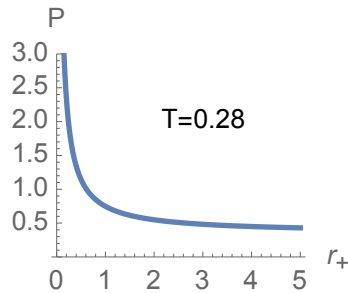


Figure 9: The figure shows P vs r_+ for the dilaton black hole for constant temperature. Here, $Q = 1, \beta = 0.1.$ and $T = 0.28.$

3.7.3 Thermodynamic stability

For the black hole to be locally stable, $C_{P,Q} > 0$. From eq.(65) this implies,

$$P > \frac{Q^2}{8\pi\beta r_+} \quad (72)$$

or,

$$-\Lambda > \frac{Q^2}{\beta r_+}. \quad (73)$$

Hence it is clear that if the black hole to be locally stable, then Λ has to be negative or has to be in anti-de Sitter space. This is very similar to the Schwarzschild anti-de Sitter black hole where it was demonstrated that $-\Lambda r_+^2 > 1$ for C_p to be positive [5]. When $C_{P,Q}$ and T are plotted against r_+ , it is clear that both are positive for the same values of r_+ as demonstrated in Fig.(10). Both $C_{P,Q}$ and T are zero when the black hole is extreme with $r_{ex} = -\frac{Q^2}{\beta\Lambda}$. Hence, provided $\Lambda < 0$, all black holes are locally stable.

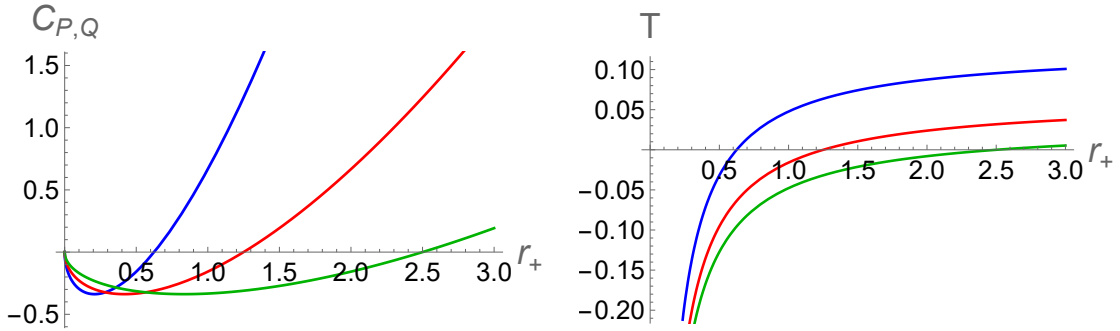


Figure 10: The figure shows the specific heat capacity $C_{P,Q}$ and Hawking temperature T vs the horizon r_+ for $N = 1$ and fixed charge. Here $Q = 0.5$, $\Lambda = -0.2$, $\gamma = 1$ and $\beta = 0.5, 1, 2$ (green, red, blue).

In order to study global stability of a black hole, one has to study the Gibbs free energy G . Note that the Gibbs free energy $G = M - TS$ for $N = 1$ does not depend on Λ as follows:

$$G = \frac{\gamma Q^2}{\sqrt{r_+}} \quad (74)$$

$$\frac{dG}{dr_+} = -\frac{\gamma Q^2}{2(r_+)^{3/2}} < 0. \quad (75)$$

Since $\frac{dG}{dr_+}$ is decreasing, it does not have a local minimum. Hence we can conclude that the black hole does not admit Van der Waals type behavior for $N = 1$ black holes. Also, $G > 0$ for all black holes and will approach zero when $T \rightarrow -\frac{\Lambda\beta}{\pi}$. Fig.(11) represent G vs T graph for $N=1$.

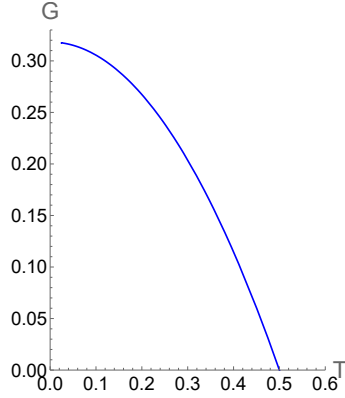


Figure 11: Gibbs free energy G versus T for $N = 1$, $Q = 0.5$, $\gamma = 1$ and $\Lambda = -1.0$.

4 Thermodynamics for the $N = \frac{2}{3}$ case

When we set $N = 2/3$ in the metric function given by eq.(9), we find that it exhibits a singularity. Numerous studies [29, 30, 35–37, 39, 40, 44, 54] have explored models of charged black holes in three-dimensional Einstein-Dilaton gravity. In these studies, cases leading to singularities are individually incorporated into the general expression for the metric function. For the dilaton black holes considered in this paper, a detailed study for $N = 2/3$ is done by Xu in reference [44]. We will adopt the metric function for $N = 2/3$ derived by Xu [44] as follows:

$$f(r) = -\frac{24Mr^{2/3}}{\gamma} - 6\beta^{4/3}\Lambda r^{2/3} \log\left(\frac{r}{\beta}\right) + 9Q^2. \quad (76)$$

Fig.(12) illustrates the behavior of this metric function with respect to the radial coordinate.

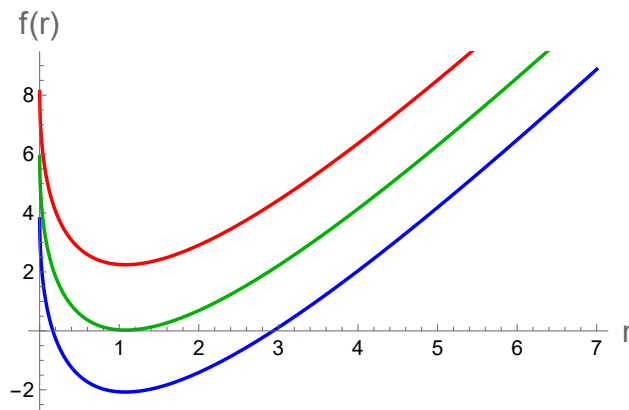


Figure 12: The metric function is represented for three different values of Q for the dilaton black hole when $N = \frac{2}{3}$. Here we choose $M = 0.3$, $\gamma = 1$, $\beta = 0.7$ and $\Lambda = -1$. The blue curve corresponds $Q = 0.65$ and is a black hole solution with two horizons. The red curve corresponds to $Q = 0.95$ and does not have horizons. The green curve corresponds $Q = 0.81$ the extremal case.

In this case the entropy is given by,

$$S = \frac{2\pi r_+ R(r_+)}{4} = \frac{\pi}{2} \gamma r_+^{1/3}. \quad (77)$$

By considering $f(r_+) = 0$, we can obtain

$$M = \frac{3\gamma Q^2}{8r_+^{2/3}} - \frac{1}{4} \gamma \beta^{4/3} \Lambda \log\left(\frac{r_+}{\beta}\right). \quad (78)$$

4.1 First Law of black hole thermodynamics for $N = \frac{2}{3}$ case

The quantities S , P , Q and β are related to the mass M as follows

$$M = \pi\gamma \left[2\beta^{4/3} P \log\left(\frac{8S^3}{\pi^3 \beta \gamma^3}\right) + \frac{3\pi\gamma^2 Q^2}{32S^2} \right]. \quad (79)$$

As for $\frac{2}{3} < N < 2$ cases, the first law of black hole thermodynamics for $N = \frac{2}{3}$ takes the form

$$dM = TdS + VdP + \Phi dQ + \Omega d\beta + \Upsilon d\gamma, \quad (80)$$

where, in the present case, the temperature is given by the expression

$$T = \left(\frac{\partial M}{\partial S} \right)_{P,Q,\beta,\gamma} = -\frac{3}{2\pi r_+} \left(\beta^{4/3} \Lambda r_+^{2/3} + Q^2 \right). \quad (81)$$

We get the same result if we use the surface gravity

$$\begin{aligned} T_H &= \frac{1}{4\pi} \left| \frac{dg_{tt}}{dt} \sqrt{-g^{tt}g^{rr}} \right|_{r_+} = -\frac{1}{2\pi(\beta^2 r_+)^{1/3}} \left(8M + 3\beta^2 \Lambda + 2\beta^2 \Lambda \log\left(\frac{r_+}{\beta}\right) \right) \\ &= -\frac{3}{2\pi r_+} \left(\beta^{4/3} \Lambda r_+^{2/3} + Q^2 \right). \end{aligned} \quad (82)$$

If $P = -\frac{\Lambda}{8\pi}$, then one can obtain the thermodynamic volume as,

$$V = \left(\frac{\partial M}{\partial P} \right)_{S,Q,\beta,\gamma} = 2\pi\gamma \beta^{4/3} \log\left(\frac{r_+}{\beta}\right). \quad (83)$$

The expression for the electric potential at the horizon gives

$$\Phi = \left(\frac{\partial M}{\partial Q} \right)_{S,P,\beta,\gamma} = \frac{3\gamma Q}{4r_+^{2/3}}. \quad (84)$$

The thermodynamic quantity Ω conjugate to the parameter β is given by,

$$\Omega = \left(\frac{\partial M}{\partial \beta} \right)_{S,P,Q,\gamma} = \frac{1}{12} \gamma \beta^{1/3} \Lambda \left[3 - 4 \log\left(\frac{r_+}{\beta}\right) \right]. \quad (85)$$

And the thermodynamic quantity Υ conjugate to the parameter γ is given by,

$$\Upsilon = \left(\frac{\partial M}{\partial \gamma} \right)_{S,P,Q,\beta} = \frac{3}{4} \beta^{4/3} \Lambda + \frac{9Q^2}{8r_+^{2/3}} - \frac{1}{4} \beta^{4/3} \Lambda \log\left(\frac{r_+}{\beta}\right). \quad (86)$$

4.2 Smarr formula

Following Smarr formula can be derived via scaling arguments given in [49]

$$(0) M = (1) \left(\frac{\partial M}{\partial S} \right) S + (-2) \left(\frac{\partial M}{\partial P} \right) P + (0) \left(\frac{\partial M}{\partial Q} \right) Q + (1) \left(\frac{\partial M}{\partial \beta} \right) \beta + \left(\frac{2}{3} \right) \left(\frac{\partial M}{\partial \gamma} \right) \gamma , \quad (87)$$

namely

$$0 = TS - 2VP + \Omega\beta + \frac{2}{3}\Upsilon\gamma . \quad (88)$$

4.3 Thermodynamical quantities

Here, we will calculate thermodynamical quantities for $N = 2/3$ case as follows:

The specific heat capacity, $C_{P,Q}$ is given by,

$$C_{P,Q} = - \frac{\pi\gamma r_+^{1/3} (Q^2 + \beta^{4/3} \Lambda r_+^{2/3})}{2(3Q^2 + \beta^{4/3} \Lambda r_+^{2/3})} . \quad (89)$$

Substituting $\Lambda = -8\pi P$ in eq.(82), one can obtain the state equation for this black hole as,

$$P = \frac{Q^2}{8\pi r_+^{2/3} \beta^{4/3}} + \frac{r_+^{1/3} T}{12\beta^{4/3}} \quad (90)$$

Since the enthalpy is given by M , which is equal to $U + PV$, one can compute U as follows:

$$U = M - PV = \frac{3\gamma Q^2}{8r_+^{2/3}} \quad (91)$$

The Gibbs free energy $G = M - TS$ is given as,

$$G = \frac{3\gamma\beta^{4/3}\Lambda}{4} - \frac{1}{4}\gamma\beta^{4/3}\Lambda \log\left(\frac{r_+}{\beta}\right) + \frac{9\gamma Q^2}{8r_+^{2/3}} . \quad (92)$$

4.4 Thermodynamics stability for $N = 2/3$ case

In this section we will analyze details of thermodynamics for the black hole with $N = 2/3$. As seen in Fig.(12), this black hole can have two horizons or degenerate horizons. When the black hole has degenerate horizons, $f(r) = f'(r) = 0$ leading to the temperature also being zero. From eq.(82), $T = 0$ when,

$$r_{ex} = \left(\frac{Q^2}{-\beta^{4/3}\Lambda} \right)^{3/2} \quad (93)$$

Also, the temperature has a maximum when the horizon radius is,

$$r_{max} = \frac{3\sqrt{3}Q^3}{\beta^2(-\Lambda)^{3/2}} \quad (94)$$

Temperature vs r_+ and $C_{P,Q}$ vs r_+ is plotted in Fig(13). One can notice that there is indeed a maximum for the temperature. Hence, black holes can exist only below the maximum temperature given by,

$$T_{max} = \frac{\beta^2(-\Lambda)^{3/2}}{\sqrt{3}\pi Q} \quad (95)$$

For a black holes to be stable locally, $C_{P,Q} > 0$. From the Fig.(13) and Fig.(14), both T and $C_{P,Q}$ are zero when the black hole is extreme at $r_+ = r_{ex}$. $C_{P,Q} \rightarrow \infty$ when $r_+ = r_{max}$ and beyond that $C_{P,Q} < 0$. Hence $C_{P,Q} > 0$ only between r_{ex} and r_{max} and that is the only region black hols are locally stable.

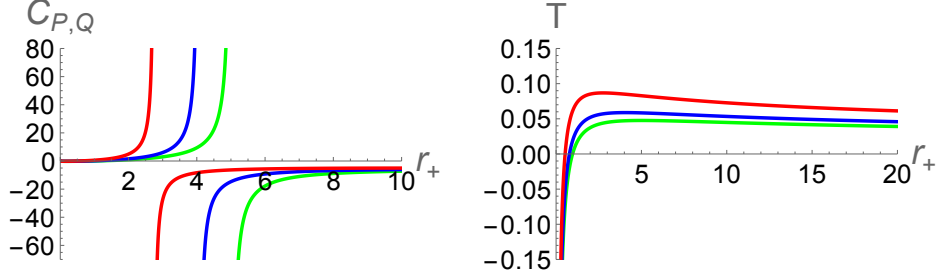


Figure 13: The specific heat capacity $C_{P,Q}$ and Hawking temperature T vs the horizon r_+ for $N = 2/3$ black hole for fixed charge. Here, $Q = 0.5, \Lambda = -1, \gamma = 1$ and $\beta = 0.486, 0.400, 0.360$ (red, blue, green).

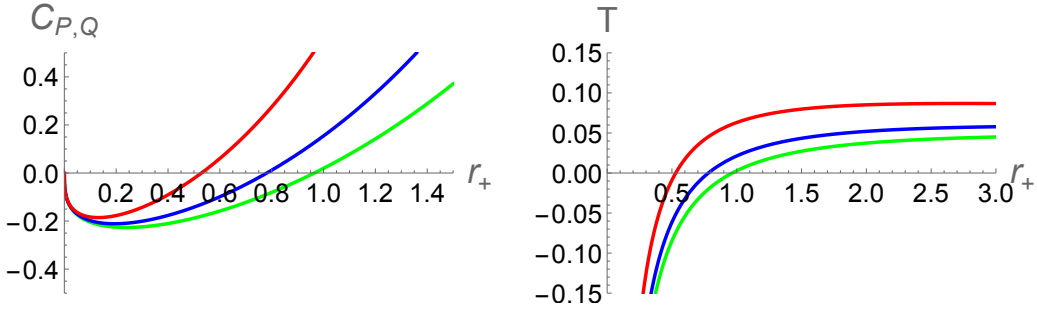


Figure 14: The specific heat capacity $C_{P,Q}$ and Hawking temperature T vs the horizon r_+ with amplified scale close to $r_+ = 0$ for the same cases as in Fig.(13)

To understand the global stability one has to study the Gibbs free energy as we did for other cases of N . In Fig.(15) we have plotted G vs T and in Fig(16) G vs r_+ and T vs r_+ . Similar to the $N = 6/7$ case, for $T < T_{max}$ there are two branches of black holes: small and large. Smaller black holes are locally stable and are preferred globally since it has lower values of G . There are no black holes beyond $T = T_{max}$. There is a first order phase transition between small black holes and the thermal AdS space at $T = T_{max}$. This is similar to the Hawking-Page phase transition in Schwarzschild-AdS black hole.

Main difference between $N = 2/3$ case and $N = 6/7$ case is that the Gibbs free energy has a minimum in $N = 2/3$ case for the range of r_+ considered.

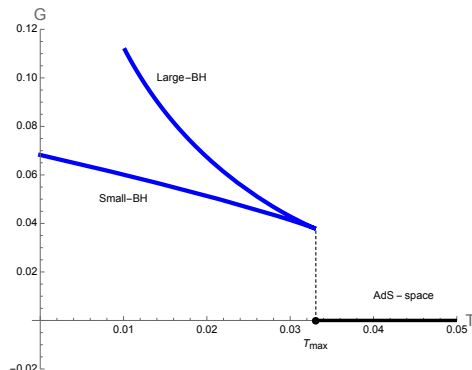


Figure 15: Gibbs free energy G is represented as a function of horizon r_+ , for fixed charge. Here, $Q = 0.5, \beta = 0.3, \gamma = 0.448, \Lambda = -1$.

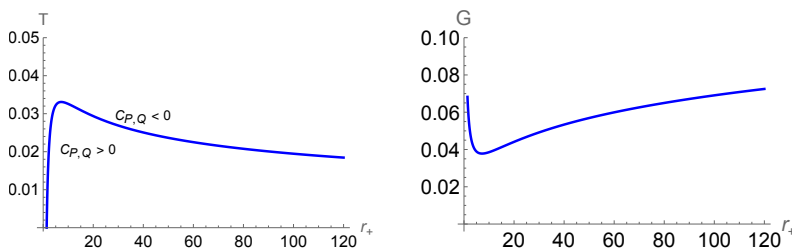


Figure 16: The figure shows the temperature T vs r and Gibbs free energy G vs r for fixed charge. Here $Q = 0.5, \beta = 0.3, \gamma = 0.448, \Lambda = -1$.

5 Joule-Thomson expansion

First, let us describe the Joule-Thomson expansion for a thermodynamical system as follows: In a Joule-Thomson experiment, gas will flow constantly along a thermally insulated tube which is divided into two compartments. There would be a porous plug in between the compartments. The gas will be at higher pressure and will move into a low pressure section. The enthalpy will remain constant along the expansion process; hence it is an iso-enthalpic process. The purpose of this experiment is to find how the temperature T varies with pressure P at constant enthalpy H , which is given by $\left(\frac{\partial T}{\partial P}\right)_H$ and is known as Joule-Thomson coefficient μ .

We will omit the derivation of the Joule-Thomson coefficient since detailed derivations are given in [52]. μ is given by,

$$\mu = \left(\frac{\partial T}{\partial P}\right)_H = \frac{1}{C_{P,Q}} \left[T \left(\frac{\partial V}{\partial T}\right)_P - V \right]. \quad (96)$$

Here, $C_{P,Q}$ is the heat capacity at constant pressure and is given in eq.(65). One can determine if the gas will cool or heat after the adiabatic expansion by evaluating the coefficient μ . If $\mu > 0$ then the temperature decreases and if $\mu < 0$ then the temperature increases. Note that in the Joule-Thomson expansion, change of pressure is negative.

For the dilaton black hole considered in this paper, we will keep charge Q constant when computing μ . Hence μ is given by,

$$\begin{aligned}\mu &= \left(\frac{\partial T}{\partial P}\right)_H = \frac{1}{C_{P,Q}} \left[T \left(\frac{\partial V}{\partial T}\right)_P - V \right] \\ &= \frac{1}{C_{P,Q}} \left[T \frac{\left(\frac{\partial V}{\partial r_+}\right)_P}{\left(\frac{\partial T}{\partial r_+}\right)_P} - V \right]\end{aligned}$$

5.1 $\frac{2}{3} < N < 2$ case

For this case, we can compute μ as,

$$\mu = \frac{1}{C_{P,Q}} \left[T \frac{\left(\frac{\partial V}{\partial r_+}\right)_P}{\left(\frac{\partial T}{\partial r_+}\right)_P} - V \right] \quad (97)$$

$$= \frac{8\beta^{2-N}r_+^{(N-1)}}{(3N-2)} \left(\frac{-3Q^2 + 8\pi P\beta^{2-N}r_+^N}{-Q^2 + 8\pi P\beta^{2-N}r_+^N} \right). \quad (98)$$

One can observe that $\mu \rightarrow \infty$ when the denominator is zero in the above expression; in fact that is where the temperature becomes zero (or where the black hole becomes extreme) at $r = r_{ex}$ given by eq.(17). $\mu = 0$ when the numerator of eq.(97) becomes zero at r_μ which is,

$$r_\mu^N = \frac{3Q^2}{(-\Lambda\beta^{2-N})} \quad (99)$$

It is clear that $r_\mu^N = 3r_{ex}^N$. In Fig.(17), the Joule-Thomson coefficient μ plotted against the horizon radius r_+ for different values of N . One can observe that for large N , μ is higher. We have omitted the region where μ goes to ∞ since that is the point where the black hole becomes extreme; r_+ smaller than that will have no black holes.

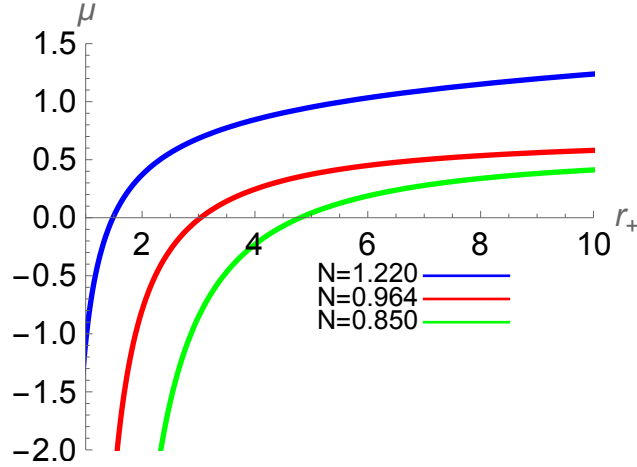


Figure 17: The figure shows the Joule-Thomson coefficient μ vs the horizon r_+ for various N values. Here $Q = 1.5, P = 1, \beta = 0.1$.

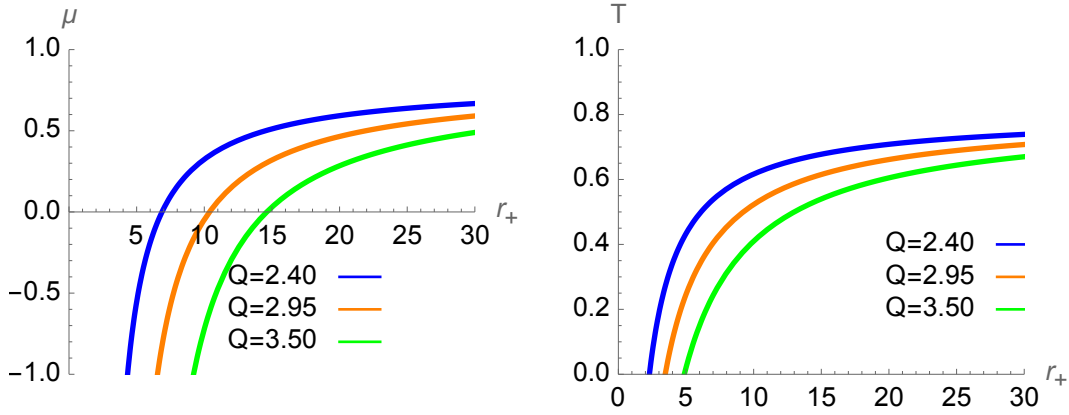


Figure 18: The figure shows the Joule-Thomson coefficient μ and Hawking temperature T vs the horizon r_+ for $N = 1$ case for fixed charge. Here $Q = 2.97, 3.97, 4.82$ and $P = 1, \beta = 0.1$.

One can define a quantity called the inversion temperature, T_i and inversion pressure, P_i when $\mu = 0$. T_i is given by,

$$T_i = V \left(\frac{\partial T}{\partial V} \right)_P = \frac{2Q^2}{N\pi r_+} \quad (100)$$

The gas will heat if one starts above the inversion temperature and will cool if one starts below the inversion temperature. The inversion pressure P_i is calculated from $\mu = 0$ via the eq.(98) as,

$$P_i = \frac{3Q^2}{8\pi\beta^{(2-N)}r_+^N} \quad (101)$$

By eliminating r_+ from both P_i and T_i , one can obtain a relation between the inversion temperature and inversion pressure as,

$$T_i = \frac{2Q^{2-\frac{2}{N}}}{N\pi} \left(\frac{8\pi\beta^{2-N}}{3} \right)^{1/N} P_i^{1/N} \quad (102)$$

In Fig.(19), T_i vs P_i is given for various N values. It is clear that T_i increases with P_i .

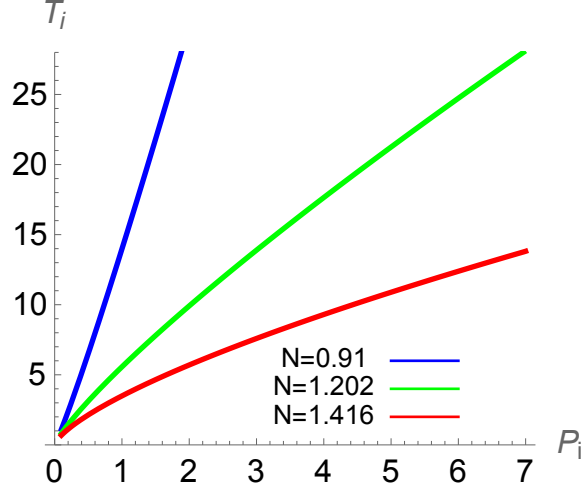


Figure 19: The figure shows the inversion curves, T_i vs P_i for the dilaton black hole for various N values. Here $\beta = 1.88$, $Q = 1.636$.

For $N = 1$ case, the above relations simplifies to,

$$T_i = \frac{2Q^2}{\pi r_+} \quad (103)$$

and

$$T_i = \frac{16\beta}{3} P_i \quad (104)$$

It can be observed that for $N = 1$ the relation is independent of the charge Q or N . It only depends on β . The inversion temperature increases monotonically with the inversion pressure P_i as shown in Fig.(20).

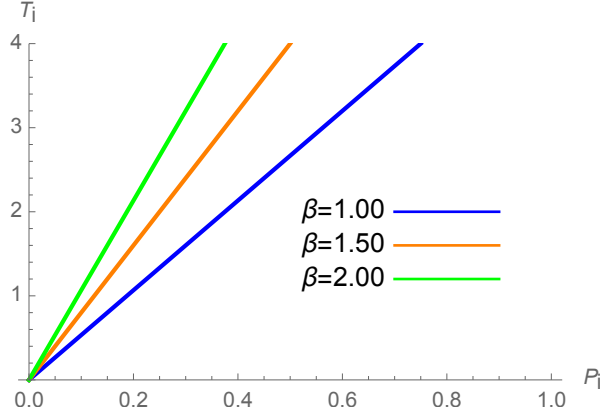


Figure 20: The figure shows the inversion curves, T_i vs P_i for the dilaton black hole for $N = 1$ case. Here $\beta = 1.00, 1.50, 2.00$.

For a given N and Q , there is only one inversion curve for the dilaton black hole. In contrast, for the Van der Waals fluid, there are two inversion curves as shown in [52]. Furthermore, the dilaton black hole does not have critical behavior similar to Van der Waals fluids as shown in section (3.1). Hence a ratio between T_i and T_c does not exist. This behavior is similar to the BTZ black hole as shown in [53].

The minimum inversion temperature, T_i^{min} is obtained at $P_i = 0$ which is,

$$T_i^{min} = 0 \tag{105}$$

Hence, T_i^{min} occurs when the black hole is extreme. This is similar to the case for the BTZ black hole [53]

Since the Joule-Thomson expansion is an isenthalpic process, we have plotted the isenthalpic curves for $N = 1$ in Fig.(21). When $\mu = 0$, i.e. $\left(\frac{\partial T}{\partial P}\right)_H = 0$, the isenthalpic curves and inversion curves intersect at $\mu = 0$ point. From Fig.(21), it is clear that the slope of the isenthalpic curve is positive above the inversion curve. Hence, if the black hole starts above the inversion curve, it will cool under this expansion. On the other hand, since the slope of the isenthalpic curve is negative below the inversion curve, the temperature of the black hole will increase if it starts below the inversion curve.

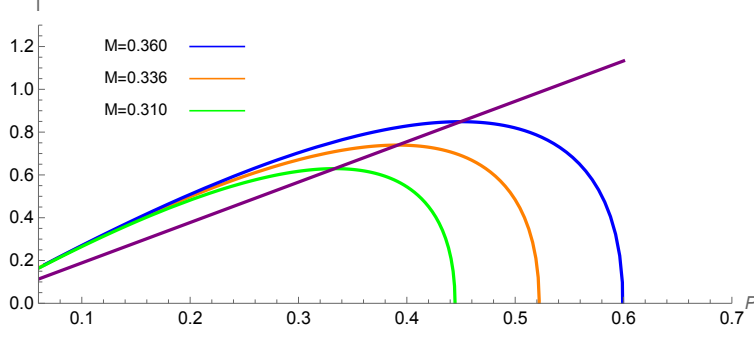


Figure 21: The figure shows isenthalpic and inversion curves for the dilaton black hole for $N = 1$ case. The isenthalpic curve is given for mass $M = 0.310, 0.336, 0.360$. The purple line is for inversion curve. Here, $Q = 1, \beta = 0.354$.

5.2 $N = 2/3$ case

For $N = 2/3$, μ is given by,

$$\mu = \frac{12\beta^{4/3}}{r^{1/3}} + \frac{4\beta^{4/3}(3q^2 + r^{2/3}\beta^{4/3}\Lambda)\text{Log}(r/\beta)}{r^{1/3}(q^2 + r^{2/3}\beta^{4/3}\Lambda)} \quad (106)$$

In Fig.(22), μ and T are plotted against the r_+ . Behavior of μ and T are very similar to the behaviour for $2/3 < N < 2$ case.

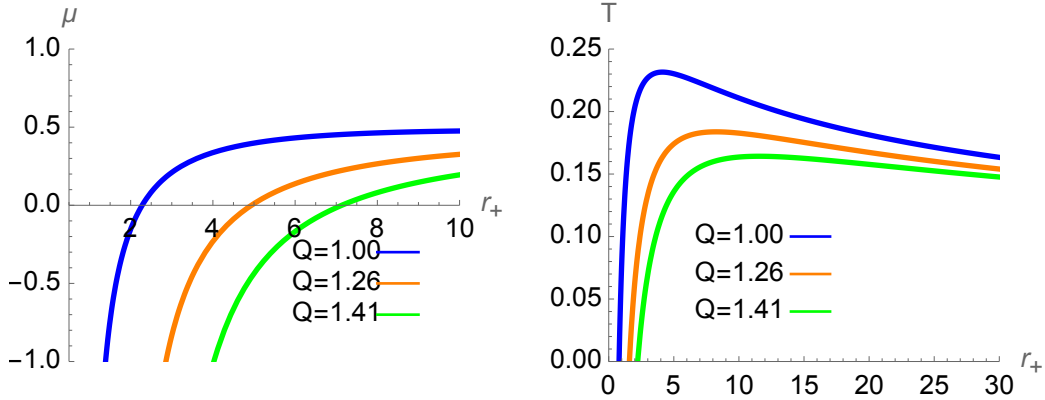


Figure 22: The figure shows the Joule-Thomson coefficient μ and Hawking temperature T vs the horizon r_+ for $N = 2/3$ case for fixed charge. Here $Q = 1.00, 1.26, 1.41$ and $P = 1, \beta = 0.1$.

Inverse temperature T_i and inverse pressure P_i are given by,

$$T_i = \frac{3Q^2 \ln(\frac{r_{\pm}}{\beta})}{\pi r_+ (3 + \ln(\frac{r_{\pm}}{\beta}))} \quad (107)$$

$$P_i = \frac{3Q^2}{8\pi r_+^{2/3} \beta^{4/3}} \left(\frac{1 + \ln(\frac{r_+}{\beta})}{3 + \ln(\frac{r_+}{\beta})} \right) \quad (108)$$

T_i vs P_i are plotted in Fig.(23). There is a significant difference in the behavior of T_i vs P_i when compared to the case for $2/3 < N < 2$. Here there are two possible values for P_i for a given T_i .

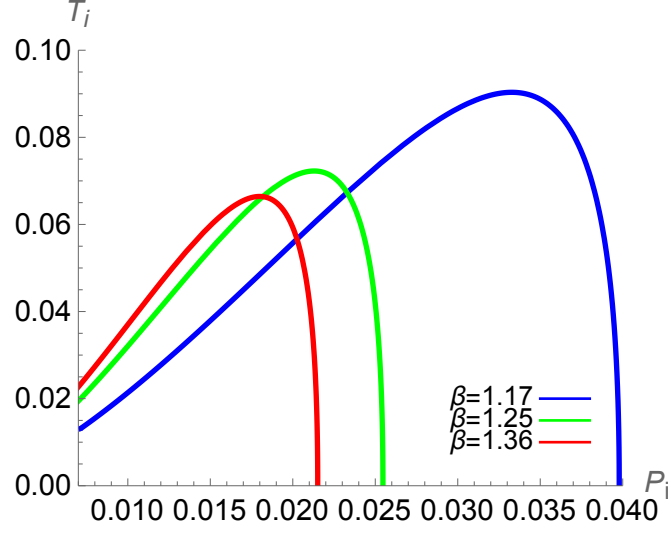


Figure 23: The figure shows the inversion curves, T_i vs P_i for the dilaton black hole for $N = 2/3$ case. Here $Q = 1$ and $\beta = 1.17, 1.25, 1.36$.

Isenthalpic curves for $N = 2/3$ is plotted in Fig.(24) and they are very similar to the $2/3 < N < 2$ case.

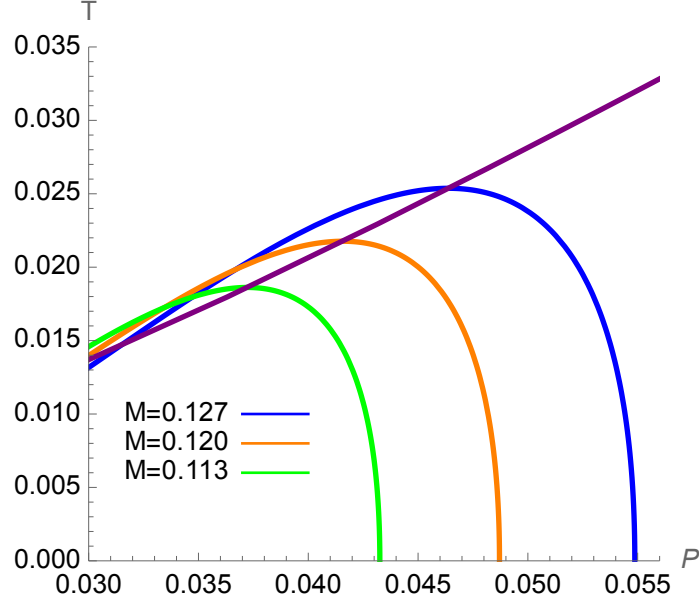


Figure 24: The figure shows isenthalpic and inversion curves for the dilaton black hole for $N = 2/3$ case. The isenthalpic curve is given for mass $M = 0.127, 0.120, 0.113$. The purple line is for inversion curve. Here, $Q = 0.395, \beta = 0.22, \gamma = 1$.

6 Reverse Isoperimetric Inequality

There is a conjecture that the isoperimetric ratio \mathcal{R} given by,

$$\mathcal{R} = \left(\frac{(D-1)V}{\omega_{D-2}} \right)^{\frac{1}{D-1}} \left(\frac{\omega_{D-2}}{A} \right)^{\frac{1}{D-2}} \quad (109)$$

will always satisfy $\mathcal{R} \geq 1$ when V is the thermodynamical volume, A is the area of the horizon and ω_{D-2} is the area of the $(D-2)$ -dimensional unit sphere [50]. Here, $D = 3$ and $\omega_1 = 2\pi$. For $2/3 < N < 2$,

$$A = 2\pi\gamma r_+^{N/2}; \quad V = \frac{4\pi\gamma\beta^{2-N}r_+^{\frac{3N}{2}-1}}{3N-2}; \quad \omega_1 = 2\pi \quad (110)$$

leading to

$$\mathcal{R} = 2\beta^{1-\frac{N}{2}} \sqrt{\frac{1}{(3N-2)\gamma} r_+^{\frac{N-2}{4}}}. \quad (111)$$

On the other hand, for $N = 2/3$,

$$A = 2\pi\gamma r_+^{1/3}; \quad V = 2\pi\gamma\beta^{4/3} \log\left(\frac{r_+}{\beta}\right) \quad (112)$$

then

$$\mathcal{R} = \frac{\sqrt{2\beta^{4/3} \log\left(\frac{r_+}{\beta}\right)}}{\gamma^{1/2} r_+^{1/3}}. \quad (113)$$

Since β is an integration constant, and its value is not determined a priori, it is not possible to say whether $\mathcal{R} \geq 1$. One may recall that in charged BTZ black holes, $\mathcal{R} < 1$ leading to a violation of the Reverse Isoperimetric Inequality [51]. Hence, inclusion of the dilaton field leads to the possibility of charged black holes in 2+1 dimensions to satisfy the Reverse Isoperimetric Inequality.

7 Conclusion

In this paper we have studied the static charged dilaton black hole in 2+1 dimensions. We have studied thermodynamics in the extended phase space where $P = -\Lambda/8\pi$. The black hole metric is given by one metric for $2/3 < N < 2$ case, and another for $N = 2/3$ case. Hence we have studied thermodynamics separately for these two groups.

We have presented first law of thermodynamics and the Smarr formula for all the black holes considered in this paper. One has to consider β and γ as thermodynamic variables in order to make the first law of thermodynamics to be consistent with the Smarr formula.

Other thermodynamical quantities such as specific heat, internal energy, Helmholtz free energy, Gibbs free energy are derived and Maxwell's relations are derived.

We will discuss thermodynamics of the black holes first:

7.1 $2/3 < N < 2$ case

We observed that the temperature T has a maximum only for $2/3 < N < 1$. For $1 \leq N < 2$, the temperature does not have a maximum. The existence of a maximum temperature does effect the specific heat capacity $C_{P,Q}$ significantly; there would be two branches for $C_{P,Q}$ when $2/3 < N < 1$ and only one branch for $1 \leq N < 2$. To understand these two groups we have studied $N = 6/7$ case and $N = 1$ case. $N = 6/7$ falls for the first group and $N = 1$ falls to the second group.

7.1.1 $N = 1$ case

For $N = 1$ case, the black hole has two horizons given the mass $M > \gamma Q \sqrt{-\beta\Lambda}$. It can have extreme black holes or naked singularities. Here, thermodynamic volume is not the geometric volume. For $N = 1$ case, the temperature T approaches $-\frac{\Lambda\beta}{\pi}$ and does not have a local maxima or a minima. Here, black holes are locally stable. In studying the Gibbs free energy, we observed that G does not have a local minimum and that there are no Van der Waals type phase transitions.

7.1.2 $N = \frac{6}{7}$ case

There is no general method to compute black hole horizons for a general N value. According to the authors in [20]. It was demonstrated that black holes existed for $2 > N > \frac{2}{3}$ for $\Lambda < 0$ and black holes with $N = \frac{6}{5}, \frac{6}{7}, \frac{4}{3}, \frac{4}{5}$ were discussed in [20]. In this paper, we have chosen $N = \frac{6}{7}$ as an example for $2/3 < N < 1$ case to analyze thermodynamics. Black holes with such an N value has the possibility to have two horizons, degenerate or no horizons depending on the mass and charge. In the extended phase space where $P = -\Lambda/(8\pi)$, the pressure has a minimum when plotted against r_+ . Hence black holes can only exist for the pressure greater than a certain value. The temperature has a maxima (T_{max}) and black holes cannot exist with temperature greater than T_{max} . Black holes are locally stable for a range of r_+ . The range lies in between when the black holes are extreme and at when the temperature is extreme. In order to understand the global stability we have studied the Gibbs free energy. Small

black holes are preferred state for smaller temperature values and the thermal AdS space is preferred after T_{max} . Hence, there is a first order phase transition between small black holes and the thermal AdS space. This is very similar to the phase transition for the Schwarzschild AdS black hole in 4 dimensions referred to as Hawking-Page phase transition.

7.1.3 $N = \frac{2}{3}$ case

Similar to $N = 6/7$ case, these black holes are locally stable for small r_+ . Observing Gibbs free energy, one could notice that there is a minimum for G . This is different from the G for $N = 6/7$ or $N = 1$ case. These black holes do have phase transitions between small black holes and the thermal AdS space similar to the $N = 6/7$ case.

7.2 Joule Thompson expansion

Joule Thomson expansion is studied in detail and Joule Thomson coefficient μ is calculated. It is clear that μ diverges at $T = 0$ where the black hole is extreme. Inversion temperature is calculated and is observed that it is proportional to the inversion pressure P_i when $2/3 < N < 2$. For $N = 2/3$ the behavior is somewhat different. There could be two values of P_i for a given T_i in this case.

Isenthalpic curves are plotted and we have discussed how the black hole heat or cool with respect to the inversion curve.

7.3 Reverse Isoperimetric Inequality

Reverse Isoperimetric Inequality is satisfied for certain values of the parameters in the theory. This behavior is unlike the charged BTZ black hole where the Reverse Isoperimetric Inequality is violated.

Charged dilaton black hole has presented with interesting behavior as opposed to the charged BTZ black hole. In extending this work, it would be interesting how adding spin to these black hole will change the thermodynamical behavior. Hence it would be interesting to study the spinning dilaton black holes presented by Chan and Mann in [21].

Acknowledgements

S. Fernando was on Sabbatical leave from Northern Kentucky University when part of this work was completed. L. Balart is supported by DIUFRO through the project: DI24-0087.

Data Availability Statement

No Data associated in the manuscript

References

- [1] J. D. Bekenstein, *Black holes and entropy*, Phys. Rev. **D7** 2333 (1973)
- [2] S. W. Hawking, *Black holes and thermodynamics*, Phys. Rev. **D13** 191 (1976)

- [3] S. W. Hawking & D.N. Page, *Thermodynamics of black holes in anti-de Sitter space*, Comm. Math. Phys. **87** 577 (1983)
- [4] D. Kastor, S. Ray, & J. Traschen, *Enthalpy and mechanics of AdS black holes*, Class. Quant. Grav. **26** 195011 (2009)
- [5] B. P. Dolan, *The cosmological constant and black hole thermodynamic potential*, Class. Quant. Grav. **28** 125020 (2011)
- [6] S. Fernando, *P-V criticality in AdS black holes of massive gravity*, Phys. Rev. **D 94** 124049 (2016)
- [7] N. Altamirano, D. Kubiznak, R. B. Mann & Z. Sherkatghanad, *Thermodynamics of rotating black holes and black rings: phase transitions and thermodynamic volume*, Galaxies **2** 89 (2014)
- [8] S. Gunasekaran, R. B. Mann, & D. Kubiznak, *Extended phase space thermodynamics for charged and rotating black holes and Born-Infeld vacuum polarization*, JHEP 11: 10 (2012)
- [9] H. Dai, Z. Zhao, and S. Zhang, *Thermodynamics phase transition of Euler-Heisenberg-AdS black hole on free energy landscape*, Nucl. Phys. B **991**, 116219 (2023).
- [10] J. Mo & W. Liu, *P-V criticality of topological black holes in Lovelock-Born-Infeld gravity*, Eur. Phys. Jour. **C 74** 2836 (2014)
- [11] S. H. Hendi, S. Panahiyan, & B. E. Panah, *Extended phase space thermodynamics and P-V criticality of black holes with Born-Infeld type nonlinear electrodynamics*, Int. Jour. Mod. Phys. **D 25** 1650010 (2016)
- [12] J. Sadeghi, B. Pourhassan, & M. Rostami, *P-V criticality of logarithmic corrected dyonic charged AdS black hole*, Phys. Rev. **D 94** 064006 (2016)
- [13] G. Li, *Effects of dark energy on P-V criticality of charged AdS black-holes*, Phys. Lett. **B735** 256 (2014)
- [14] J. Mo, G. Li, & X. Xu, *Effects of power-law Maxwell field on the Van der Waals like phase transition of higher dimensional dilaton black holes*, Phys. Rev. **D 93** 084041 (2016)
- [15] M. Zhang & W Liu, *Coexistent physics of massive black holes in the phase transitions*, arXiv: 1610.03648
- [16] J. Mo, G. Li, & X. Xu, *Combined effects of $f(R)$ gravity and conformally invariant Maxwell field on the extended phase space thermodynamics of higher-dimensional black holes*, Eur. Phys. Jour. **C 76** 545 (2016)
- [17] R Cai, L. Cao, & R. Yang, *P-V criticality in the extended phase space of Gauss-Bonnet black holes in AdS space* JHEP:1309 005 (2013)
- [18] D. Kubiznak, R. B. Mann, & M. Teo, *Black hole chemistry: thermodynamics with Lambda*, Class. Quant. Grav. **34** 063001 (2017)
- [19] M. Banados, C. Teitelboim and J. Zanelli, *The Black hole in three-dimensional space-time*, Phys. Rev. Lett. **69**, 1849-1851 (1992)

- [20] K. C. K. Chan and R. B. Mann, *Static charged black holes in (2+1)-dimensional dilaton gravity*, Phys. Rev. D **50**, 6385 (1994) [erratum: Phys. Rev. D **52**, 2600 (1995)]
- [21] K. C. K. Chan and R. B. Mann, *Spinning black holes in (2+1)-dimensional string and dilaton gravity*, Phys. Lett. B **371**, 199-205 (1996)
- [22] P. M. Sa, A. Kleber and J. P. S. Lemos, *Black holes in three-dimensional dilaton gravity theories*, Class. Quant. Grav. **13**, 125-138 (1996)
- [23] K. C. K. Chan, *Modifications of the BTZ black hole by a dilaton / scalar*, Phys. Rev. D **55**, 3564-3574 (1997)
- [24] Y. Kiem and D. Park, *Magnetically charged solutions via an analog of the electric - magnetic duality in (2+1)-dimensional gravity theories*, Phys. Rev. D **55**, 6112-6115 (1997)
- [25] T. Koikawa, T. Maki and A. Nakamura, *Magnetic solutions to (2+1)-dimensional gravity with dilaton field*, Phys. Lett. B **414**, 45-51 (1997)
- [26] P. M. Sa and J. P. S. Lemos, *Stationary black holes in a generalized three-dimensional theory of gravity*, Phys. Lett. B **423**, 49-53 (1998)
- [27] S. Fernando, *Spinning charged solutions in (2+1)-dimensional Einstein-Maxwell Dilaton gravity*, Phys. Lett. B **468**, 201-207 (1999)
- [28] T. Maki, *A new family of exact solutions in 2+1 dimensional Einstein-Maxwell-dilaton theory*, Prog. Theor. Phys. **123**, 355-367 (2010)
- [29] M. Dehghani, *Thermodynamics of (2+1)-dimensional black holes in Einstein-Maxwell-dilaton gravity*, Phys. Rev. D **96**, no.4, 044014 (2017)
- [30] M. Dehghani, "Thermodynamic properties of charged three-dimensional black holes in the scalar-tensor gravity theory," Phys. Rev. D **97**, no.4, 044030 (2018).
- [31] M. Cataldo and A. Garcia, *Three dimensional black hole coupled to the Born-Infeld electrodynamics*, Phys. Lett. B **456**, 28-33 (1999)
- [32] M. Cataldo, N. Cruz, S. del Campo and A. Garcia, *(2+1)-dimensional black hole with Coulomb - like field*, Phys. Lett. B **484**, 154 (2000)
- [33] O. Gurtug, S. H. Mazharimousavi and M. Halilsoy, *2+1-dimensional electrically charged black holes in Einstein - power Maxwell Theory*, Phys. Rev. D **85**, 104004 (2012)
- [34] R. Yamazaki and D. Ida, *Black holes in three-dimensional Einstein-Born-Infeld dilaton theory*, Phys. Rev. D **64**, 024009 (2001)
- [35] M. Dehghani, "Thermodynamics of novel dilatonic BTZ black holes coupled to Born-Infeld electrodynamics," Phys. Rev. D **99**, no.2, 024001 (2019).
- [36] M. Dehghani, "Black hole thermodynamics in (2 + 1)-dimensional scalar-tensor-Born-Infeld theory," Eur. Phys. J. C **82**, no.4, 367 (2022).

- [37] M. Dehghani, “Thermodynamics of novel scalar–tensor–Born–Infeld black holes,” *Eur. Phys. J. C* **83**, no.11, 987 (2023).
- [38] M. Dehghani, *Three-dimensional black holes with scalar hair coupled to a Maxwell-like electrodynamics*, *Mod. Phys. Lett. A* **37**, no.30, 2250205 (2022)
- [39] M. Dehghani, “Nonlinearly charged three-dimensional black holes in the Einstein-dilaton gravity theory,” *Eur. Phys. J. Plus* **133**, no.11, 474 (2018).
- [40] M. Dehghani, “Three-dimensional scalar-tensor black holes with conformally invariant electrodynamics,” *Phys. Rev. D* **100**, no.8, 084019 (2019).
- [41] Y. Younesizadeh, A. A. Ahmad, A. H. Ahmed, F. Younesizadeh and M. Ebrahimkhas, *A new black hole solution in dilaton gravity inspired by power-law electrodynamics*, *Int. J. Mod. Phys. A* **34**, no.35, 1950239 (2020)
- [42] G. Mandal, A. M. Sengupta and S. R. Wadia, *Classical solutions of two-dimensional string theory*, *Mod. Phys. Lett. A* **6**, 1685-1692 (1991)
- [43] G. T. Horowitz, *The dark side of string theory: Black holes and black strings*, [arXiv:hep-th/9210119 [hep-th]]
- [44] W. Xu, “Charged dilaton solutions and black hole formation in three dimensions,” *Eur. Phys. J. C* **79**, no.8, 642 (2019).
- [45] M. Dehghani, *Nonlinearly charged scalar-tensor black holes in (2+1) dimensions*, *Phys. Rev. D* **99**, no.10, 104036 (2019)
- [46] M. Dehghani, *Thermodynamics of new black hole solutions in the Einstein–Maxwell-dilaton gravity*, *Int. J. Mod. Phys. D* **27**, no.07, 1850073 (2018)
- [47] D. Kubiznak and R. B. Mann, *P-V criticality of charged AdS black holes*, *JHEP* **07**, 033 (2012)
- [48] C. Martinez, C. Teitelboim and J. Zanelli, *Charged rotating black hole in three space-time dimensions*, *Phys. Rev. D* **61**, 104013 (2000)
- [49] D. Kastor, S. Ray and J. Traschen, *Enthalpy and the Mechanics of AdS Black Holes*, *Class. Quant. Grav.* **26**, 195011 (2009)
- [50] M. Cvetic, G. W. Gibbons, D. Kubiznak, and C. N. Pope, *Black hole enthalpy and an entropy inequality for the thermodynamic volume*, *Phys. Rev. D* **84** 024037 (2011)
- [51] A. M. Frassino, R.B. Mann, and J. R. Mureika, *Lower-dimensional black hole chemistry*, *Phys. Rev. D* **92** 124069 (2015)
- [52] Ö. Ökcü and E. Aydine, *Joule-Thomson expansion of charged AdS black holes*, *Eur. Phys. J. C* **77**, no.1, 24 (2017)
- [53] J. Liang, B. Mu, and P. Wang, *Joule-Thomson expansion of lower-dimensional black hole*, *Phys. Rev. D* **104** 12, 124003 (2021)
- [54] M. Dehghani, “Black hole thermodynamics in the Brans–Dicke–Maxwell theory,” *Eur. Phys. J. C* **83**, no.8, 734 (2023).